Journal of Hydrology (2008) **356**, 199–208

available at www.sciencedirect.com

ScienceDirect

journal homepage: www.elsevier.com/locate/jhydrol

Topography representation methods for improving evaporation simulation in groundwater modeling

H.T. Li [a,*], W. Kinzelbach [a], P. Brunner [b], W.P. Li [c], X.G. Dong [d]

[a] *Institute of Environmental Engineering (IfU), ETH Zurich, CH-8093 Zurich, Switzerland*
[b] *School of Chemistry, Physics and Earth Sciences, Flinders University, 5001, Australia*
[c] *China Institute of Geo-Environmental Monitoring, Beijing 100081, China*
[d] *Xinjiang Agricultural University, Urumqi 830052, China*

Received 18 August 2007; received in revised form 2 April 2008; accepted 7 April 2008

KEYWORDS
Evaporation;
Groundwater modeling;
Digital elevation model

Summary In a groundwater model, surface elevations which are used in simulating the phreatic evaporation process are usually incorporated as spatially constant over discretized cells. Traditionally, a modeler obtains the data for surface elevations from point data or a digital elevation model (DEM) by means of extrapolation or interpolation. In this way, a smoothing error of surface elevations is introduced, which via the depth to groundwater propagates into evaporation simulation. As a consequence, the evaporation simulation results can be biased.

In order to explore the influence of surface elevations on evaporation simulation, three alternative methods of representation of topography in calculating evaporation were studied. The first one is a traditional method which uses cell-wise constant elevations obtained by averaging surface elevations from the DEM with higher resolution for the corresponding model cells. The second one retains some information on the sub-pixel statistics of surface elevations from the DEM by a perturbation approach, calculating the second order first moment of evaporation with a Taylor expansion. In the third method a finer discretization is used to represent the topography in calculating evaporation than is used to compute global groundwater flow. This allows to take into account the smaller scale variations of the surface elevation as given in the high resolution DEM data. For all the three methods, two different evaporation functions, a linear segment function and an exponential function have been used individually.

In this paper, a groundwater model with a discretization of 500×500 m has been established while DEM data with a resolution of 90×90 m are available and resampled to 100×100 m cells for convenience of model input. The evaporation rates from a groundwater model with a discretization of 100×100 m, which has the same spatial distribution pattern of hydraulic parameters as the 500×500 m model, is taken as validation data.

* Corresponding author. Tel.: +41 44 633 3082; fax: +41 44 633 1061.
E-mail address: li@ifu.baug.ethz.ch (H.T. Li).

0022-1694/$ - see front matter
doi:10.1016/j.jhydrol.2008.04.009

The comparisons of evaporation rates were carried out on different averaging scales ranging from 500 m to 2 km. The compared evaporation rates for each scale are obtained by summing up the corresponding evaporation rates from the 500×500 m model and the 100×100 m model. It is shown that the third method, which uses a finer resolution of topography in the evaporation calculation, yields the best results no matter which evaporation function is used. It is also seen that the correlation between the evaporation rates from the 500×500 m model and the 100×100 m model increases and values converge when comparing the evaporation results on an increasingly coarser scale, independently of the selected method and evaporation function.

Introduction

In arid and semi-arid regions, a significant amount of groundwater can be evaporated if the groundwater table is sufficiently close to the surface. In many cases, a high groundwater table is the consequence of intensive irrigation without an adequate drainage system. Evaporation of groundwater does not only reduce the available water resources, it also triggers an accumulation of salts in the soil column. The impact of soil salinity on crops results in economic losses. The reduction of available water resources can pose a serious threat to natural ecosystems such as wetlands. In order to quantify direct evaporation and to develop strategies for sustainable development, a groundwater model can help.

One of the popular groundwater modeling codes is the modular three-dimensional finite-difference ground-water model (MODFLOW). In some versions of MODFLOW (e.g. MODFLOW 88, MODFLOW 96 and MODFLOW 2000), evaporation and transpiration are lumped together and simulated in one term that increases with rising water tables (McDonald and Harbaugh, 1988, 1996; Banta, 2000). However, in some cases this may not be appropriate, as transpiration depends on more parameters than just the depth to groundwater. More sophisticated ways to treat both terms are presented in Maddock and Baird (2003) and Bauer et al. (2006) for the riparian environment and Schmid et al. (2006) for irrigated areas. In this study the evapotranspiration package (ETS package) of MODFLOW 2000 has been used to simulate evaporation instead of evapotranspiration.

In the ETS package of MODFLOW 2000, the determinative factors are the maximum evaporation rate, the depth to groundwater which is defined as the difference between surface elevation and groundwater table elevation and the extinction depth which indicates the depth to groundwater at which the evaporation rate equals zero (Banta, 2000). The maximum evaporation rates can be calculated from standard meteorological data such as temperature, wind-speed and relative humidity (Owens, 1934; Alty, 1933; American Society of Civil Engineers Task Committee on Hydrology Handbook, 1996). The evaporation rates through the soil column at different depths to groundwater can be estimated by interpreting the distribution of stable isotopes in the unsaturated zone (Craig and Gorden, 1965; Zimmermann et al., 1967; Barnes and Allison, 1988). The extinction depth can roughly be estimated by comparing such evaporation measurements at different depths to groundwater. Finally, the depth to groundwater is of crucial importance. As the groundwater table often varies more smoothly than topography, the variability of evaporation over a given area is to a high degree related to the variability of the surface elevation.

In this contribution we discuss the influence of the representation of topography on the simulation of phreatic evaporation. We illustrate that reducing the spatial resolution of a digital elevation model (DEM) data for a groundwater model can lead to a smoothing error that propagates via the depth to groundwater into the evaporation simulation. The goal of this study is to reduce this smoothing error by incorporating the sub-cell elevation information in the evaporation simulation. We discuss the approaches on the basis of two different evaporation functions relating the depth to groundwater and evaporation rates. One is the linear segment evaporation function and the other the exponential evaporation function.

Representation of topography in evaporation simulation

Traditionally, point data of surface elevations were collected and interpolated in order to obtain the surface elevations for simulation. A big shortcoming of this method is local inaccuracy since the number of point data is limited. With the development of space techniques, digital elevation model (DEM) data with increasingly higher resolution are available, e.g. the SRTM model (Rabus et al., 2003). Methods of developing DEM and its application in topographic mapping are presented by Zebker and Goldstein (1986), Wang (1990), and Hellweger and Maidment (1997).

For groundwater simulation on a basin scale, the spatial resolution of the available DEMs is usually too fine and has to be adjusted to spatial resolution applied in the groundwater model by an averaging method (Fig. 1). The cell on the left

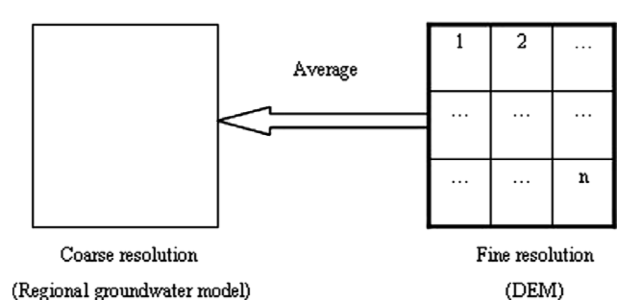

Figure 1 Sketch of averaging DEM values for the surface elevation in a groundwater model cell.

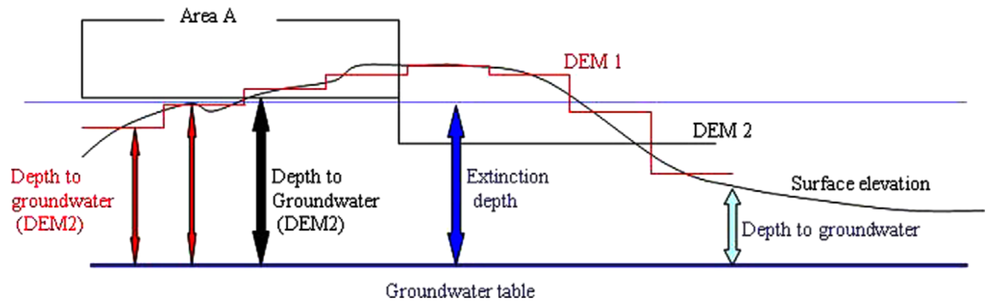

Figure 2 Section view of evaporation. Two digital elevation models featuring different spatial resolutions are plotted along a continuous topography. For the configuration shown in this figure, evaporation does not occur in area A if it is calculated in a model using the coarse DEM (DEM2).

hand side of Fig. 1 represents a groundwater model cell which contains n DEM cells shown on the right hand side of Fig. 1. The surface elevation of a model cell is calculated by using an averaging algorithm

$$\bar{s} = f(s_1, s_2, s_3, \ldots, s_n) \quad (1)$$

where $\bar{s}$ is the surface elevation for a model cell (L); s_i is the ith surface elevation in a DEM cell (L); and f is an averaging function (–).

A scale problem occurs when we try to feed finer DEM elevation data into a coarser grid of the regional groundwater model by the method shown in Fig. 1. The problem is illustrated in Fig. 2. The black curve represents the real topography. The red line[1] represents a DEM with a fine resolution (DEM1). Evaporation occurs in some cells in area A if we calculate the depth to groundwater on the basis and spatial resolution of DEM1 (red line). However, if the depth to groundwater is calculated on the basis of DEM2 (black straight line) no evaporation occurs as the depth to groundwater is larger than the extinction depth. Obviously, the evaporation rates calculated with the two different DEMs in area A are different.

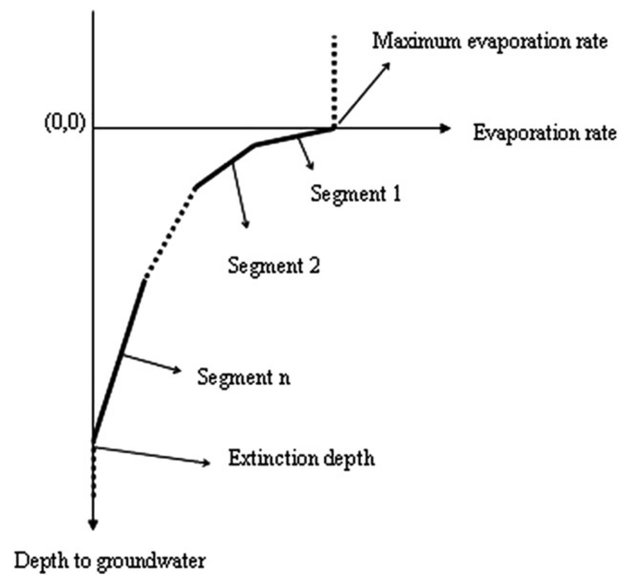

Figure 3 Sketch of linear segment evaporation.

Evaporation functions

Studies on evaporation functions are presented by Philip (1957), Gardner (1958), and Ripple et al. (1972). In a simplified evaporation function, evaporation from groundwater can be expressed as a function of depth to groundwater and parameterized by the following parameters:

s is the surface elevation (L); h is the elevation of groundwater table (L); d is the depth to groundwater (L) ($d = s - h$); d_e is the extinction depth (L); and E_{max} is the maximum evaporation rate (LT^{-1}).

Linear segment function

In the ETS package of MODFLOW 2000 (Banta, 2000), it is assumed that the relation between the depth to groundwater and the evaporation rate is non-linear. This package allows to split up the relation between depth to groundwater and evaporation rate into a series of linear segments (Fig. 3). The linear segment evaporation function can be expressed by

$$E_i = \begin{cases} E_{\max}, & d \leqslant 0 \\ E_{\max,i} + \frac{E_{\max,i+1} - E_{\max,i}}{d_{i+1} - d_i}(d - d_i), & d_i < d < d_{i+1} \\ 0, & d \geqslant d_e \end{cases} \quad (2)$$

where E_i is the evaporation rate of a model cell, where the depth to groundwater lies in the range of the ith segment (LT^{-1}); $E_{\max,i}$ is the maximum evaporation rate of the ith segment (LT^{-1}); and d_i is the depth to groundwater, where the evaporation rate reaches the maximum in the ith segment (L).

Exponential function

As an alternative to the linear segment function, exponential functions can be used to depict the relation between evaporation rate and depth to groundwater (Philip, 1957; Coudrain-Ribstein et al., 1998). An example for such a parameterization is shown in the below equation and plotted in Fig. 4

$$E = \begin{cases} E_{\max}, & d \leqslant 0 \\ E_{\max} \times \exp\left(-a\frac{d}{d_e}\right), & d > 0 \end{cases} \quad (3)$$

[1] For interpretation of color in Fig. 2, the reader is referred to the web version of this article.

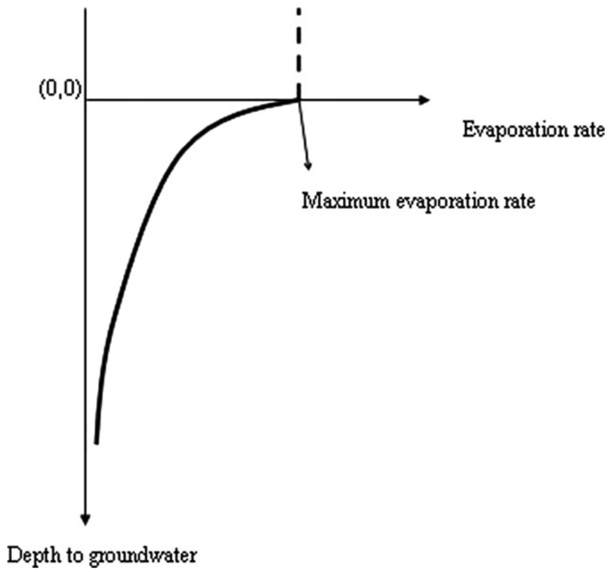

Figure 4 Sketch of exponential evaporation function.

Incorporation of the functions in MODFLOW 2000

The linear segment function is available in the current version of MODFLOW 2000 (Banta, 2000). In order to simulate an exponential relation between depth to groundwater and evaporation in MODFLOW, the code of MODFLOW 2000 has to be modified. From the equation of exponential evaporation function and curve, evaporation is larger than zero no matter how deep the depth to groundwater is. To be consistent with the linear segment function, an extinction depth can be introduced in the exponential function which is not shown in Fig. 4.

Methods for representation of topography in evaporation simulation

In order to explore the influence of the representation of topography on the simulation of phreatic evaporation, we compare three methods of representation of topography in evaporation simulation. One method is the traditional method using the arithmetic average of sub-grid elevations. The second method corrects the averaged elevation by the second order first moment method, obtained from a Taylor series expansion. The last method uses a much finer grid to calculate evaporation than is used for the global groundwater flow simulation.

Traditional method

The first method deals with the surface elevation in a traditional way. As illustrated in the second section of this paper, it uses the arithmetically averaged surface elevation for the evaporation simulation. As shown in Fig. 2, a smoothing error could occur if we use a coarser DEM in stead of a finer DEM in evaporation calculation. It is clear that this error will be significant, if the variation in elevation is comparable to the extinction depth.

Correction with Taylor series expansion

Arithmetic averaging of the surface elevation introduces error in evaporation simulation due to non-linearity of the evaporation function. This can be partially prevented by correcting the average surface elevations using the second order-first moment method. It allows to incorporate subcell elevation information. For simplicity of presentation it is applied to the exponential evaporation function here.

By expanding Eq. (3) into a Taylor series around the average depth to groundwater d_0 of a groundwater model cell, the following equation is obtained:

$$E(d) = \begin{cases} E_{\max}, & d \leqslant 0 \\ E(d_0) + E'(d_0)(d - d_0) & d > 0 \\ \quad + \frac{1}{2}E''(d_0)(d - d_0)^2 + \cdots, & \end{cases} \tag{4}$$

As a first approximation, the third and higher orders of the expansion are neglected. After substituting Eq. (3) into Eq. (4), the following equation is obtained:

$$E(d) = \begin{cases} E_{\max}, & d \leqslant 0 \\ E(d_0)\left(1 - \frac{a}{d_e}(d - d_0) + \frac{a^2}{d_e^2}(d - d_0)^2\right), & d > 0 \end{cases} \tag{5}$$

By applying Eq. (5) to all the sub-cells in the right hand side map of Fig. 1 and summing up the evaporation rates for the corresponding model cell in the left hand side map of Fig. 1, the total evaporation is thus given by Eq. (6) for a single groundwater model cell

$$E_p|_{\text{model cell}} = E_p(d_0) \sum_{i=1}^{n} \left(1 - \frac{a}{d_e}(d_i - d_0) + \frac{a^2}{d_e^2}(d_i - d_0)^2\right) \tag{6}$$

Eq. (6) can be abbreviated as

$$E_p|_{\text{model cell}} = \lambda \times E_p(d_0) \tag{7}$$

where λ is a coefficient which is given by

$$\lambda = \sum_{i=1}^{n} \left(1 + \frac{a^2}{d_e^2}(d_i^2 - d_0^2)\right) = n\left(1 + \frac{a^2}{d_e^2}\mathrm{Var}(d)\right) \tag{8}$$

Assuming the groundwater heads to be constant over the model cell, Eq. (8) can be transformed into

$$\lambda = n\left(1 + \frac{a^2}{d_e^2}\mathrm{Var}(s)\right) \tag{9}$$

This formula allows a correction of the evaporation rate only based on the variance of the topography. The correction is applied iteratively with the simulation of the groundwater model.

Higher resolution for evaporation

In this method, we also create sub-cells in each groundwater model cell as shown in the right hand side map of Fig. 1 and specify surface elevations for each sub-cell. Evaporation rates for each sub-cell are calculated individually assuming that the groundwater head in every sub-cell is identical to the groundwater head in the corresponding model cell. The resulting rates are summed up to obtain the evaporation rate for the model cell. This evaporation rate is used iteratively in the global groundwater flow simulation

$$E_p\big|_{\text{model cell}} = \sum_{i=1}^{n} \left(E_{p,i}\big|_{\text{sub-cell}} \right) \tag{10}$$

Application

The different methods are tested in a case study. The project area is the Yanqi basin in Xinjiang, China. The Yanqi basin is located in the northwestern part of China. The climate is continental and dry. The annual amount of precipitation is about 50 mm. Compared to the potential evaporation, the precipitation is negligible. The Kaidu River is the biggest river in the basin. It originates from the mountains in the northwest and terminates in the Bostan Lake. The outflow of Bostan Lake is the Kongque River which connects the Yanqi basin and the so-called green corridor in the downstream. The depths to groundwater in the basin are mainly between 0.5 and 3 m. A huge amount of water is unproductively evaporated while the downstream system faces a big problem of water scarcity. The correct simulation of evaporation is obviously crucial for a model which is supposed to be the basis for water resources management. In this study, we are interested in the phreatic evaporation on the land area.

As stated by Brunner (2005), the maximum evaporation rate (E_{max}) is 1400 mm a^{-1}, the extinction depth (d_e) is 2.58 m. In order to perform the different versions of evaporation simulation, the code, MODFLOW 2000 (Harbaugh et al., 2000), was modified correspondingly. The available DEM has a resolution of 90 × 90 m and is resampled to 100 × 100 m for a more convenient model input. The modeled area is indicated by the solid black line (Fig. 5). It includes the lake area (dashed line in Fig. 5). The groundwater model was discretized into cells of size 500 × 500 m horizontally and four layers vertically. The groundwater model has 22,850 active cells not including the lake cells. The lake is simulated by the Lake package provided in MODFLOW 2000 (Merritt and Konikow, 2000). While the Taylor expansion method uses the exponential function only, the other two methods use both the linear segment function and the exponential function. The two evaporation functions, which are used in this study, are plotted in Fig. 6. For all calculations, the spatial distributions of model input parameters are identical except for the DEMs (Table 1).

Comparison of evaporation results

In order to compare the evaporation rates from different methods and evaporation functions, the evaporation result from a groundwater model with a discretization of 100 × 100 m was chosen as validation data. The model was run both with the linear segment evaporation function and the exponential evaporation function individually. Apart from the DEM, the 100 × 100 m model has the same spatial distribution pattern of hydraulic parameters as the 500 × 500 model.

Linear segment function

The linear segment evaporation function is only applied to the traditional method and the higher resolution method of topography representation in evaporation simulation. In order to compare the evaporation rates on the same scale, the evaporation rates of the 100 × 100 m model are summed up over each 500 × 500 m cell. From the evaporation rate comparison (Fig. 7), we can see that the correlation coefficient of evaporation rates from the 100 × 100 m model and from the 500 × 500 m model is 0.68 when we use the traditional method. It increases to 0.81 when we use the higher resolution method.

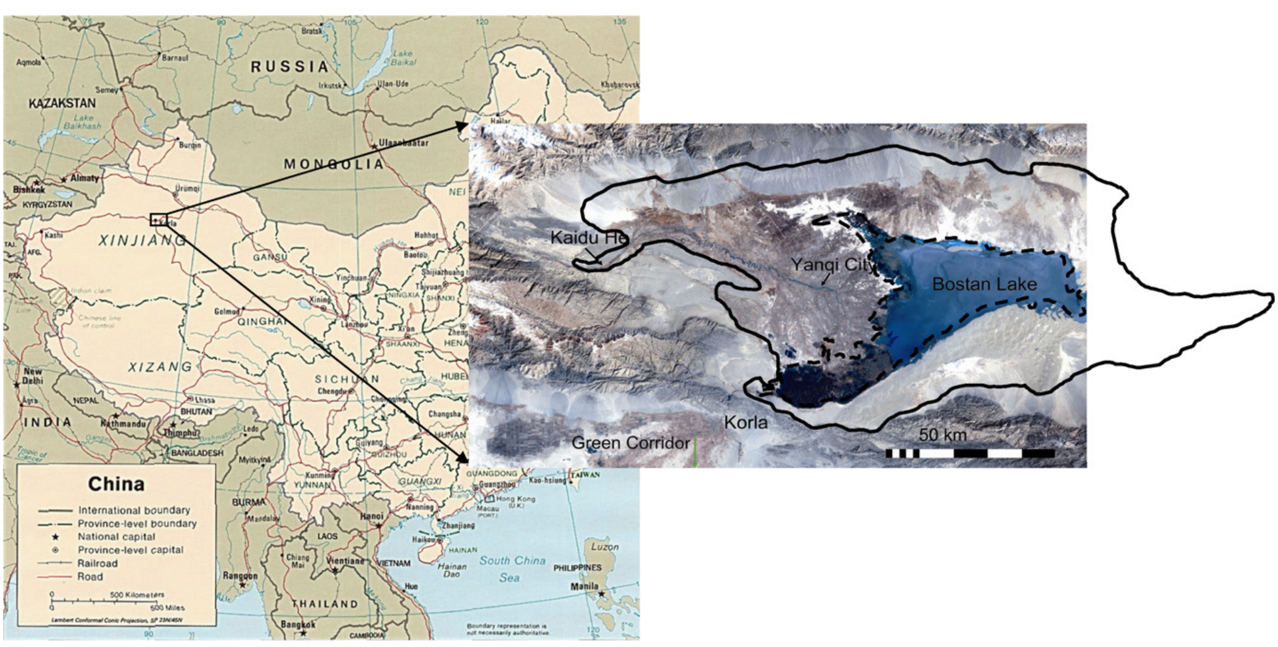

Figure 5 Sketch map of the Yanqi basin.

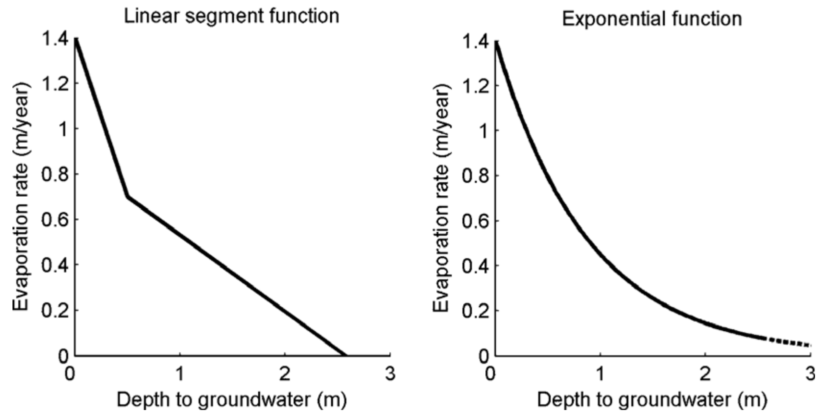

Figure 6 Curves of linear segment function and exponential function used in the study. For the exponential function, $a = 2.93$. If the depth to groundwater is larger than 2.58 m evaporation is set to zero in both functions.

Table 1 Table of resolutions of flow model and DEM in different topography representation methods

Topography representation method	Resolution of model (m)	Resolution of input DEM (m)
Traditional method	500 × 500	500 × 500[a]
Taylor expansion method	500 × 500	100 × 100
Higher resolution method	500 × 500	100 × 100

[a] 500 × 500 m DEM are the arithmetically averaged values from the 100 × 100 m DEM.

From the left hand side map of Fig. 7, we can see that the evaporation rates of the 500 × 500 m model nearly reach the maximum in some cells while those summed up from 100 × 100 m do not. This is due to bias in the simulated heads in the 500 × 500 m model. The bias results from the inaccuracy of the DEM (after averaging). By using the higher resolution method, it can be removed to a large degree (see map on the right hand side of Fig. 7).

The comparisons show that by taking the sub-cell elevation information into account the higher resolution method of topography representation behaves better than the traditional method although the correlation is still not satisfactory. However, if we compare the evaporation results on a coarser scale the correlation increases. Fig. 8 shows the evaporation comparison on the basis of 1 × 1 km and 2 × 2 km cells, respectively. In both cases, the evaporation rate in a cell is on one hand the sum from the 500 × 500 m model cells and on the other hand the sum from the 100 × 100 m model cells which are contained in the corresponding coarser cell. It is seen that the correlation reaches 0.9 when we compare the evaporation results on the basis of 2 × 2 km cells (Table 2).

Exponential function

The exponential evaporation function is applied with all the three methods. The evaporation results of the 100 × 100 m model are also summed up over each 500 × 500 m cell. From the comparison (Fig. 9), the correlation coefficient is 0.67 when we use the traditional method. It increases to 0.78 in the Taylor expansion method and to 0.81 in the higher resolution method. It is also can be seen that the bias in simulated groundwater heads is removed to a certain degree by the Taylor expansion method and higher resolution method.

In comparison to the higher resolution method, the Taylor expansion method is also an alternative for increasing the accuracy of evaporation simulation in groundwater

Table 2 Correlation coefficients of evaporation rates originating from the 100 × 100 m model and the 500 × 500 m model on different scales using the linear segment evaporation function

Method	Traditional method			Higher resolution method		
Scale	500	1 km	2 km	500 m	1 km	2 km
Correlation coefficient (R)	0.68	0.85	0.92	0.81	0.89	0.92

Table 3 Correlation coefficients of evaporation rates originating from the 100 × 100 m model and the 500 × 500 m model on different scales using the exponential evaporation function

Method	Traditional method			Taylor expansion method			Higher resolution method		
Scale	500 m	1 km	2 km	500 m	1 km	2 km	500 m	1 km	2 km
Correlation coefficient (R)	0.67	0.84	0.90	0.78	0.86	0.90	0.81	0.89	0.92

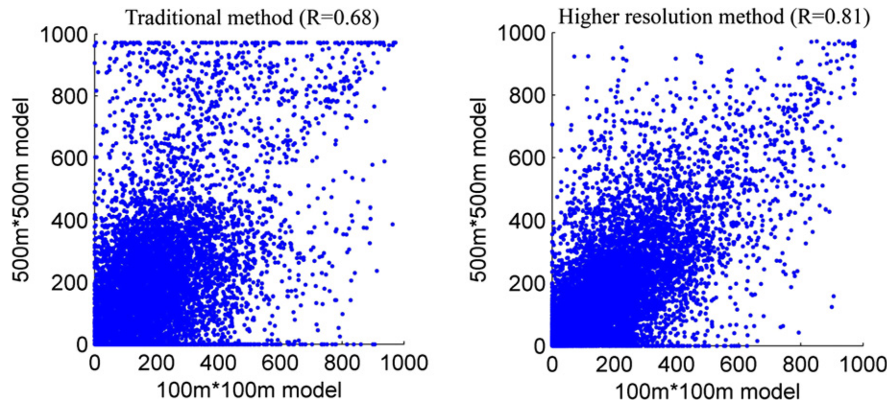

Figure 7 Comparison of evaporation rates ($m^3\,d^{-1}$ per cell) using the linear segment evaporation function on the basis of 500×500 m cells. The evaporation rates on the *x*-axis are the sums from evaporation results of the 100×100 m model for the corresponding cell in the 500×500 m model (evaporation from the lake is not included).

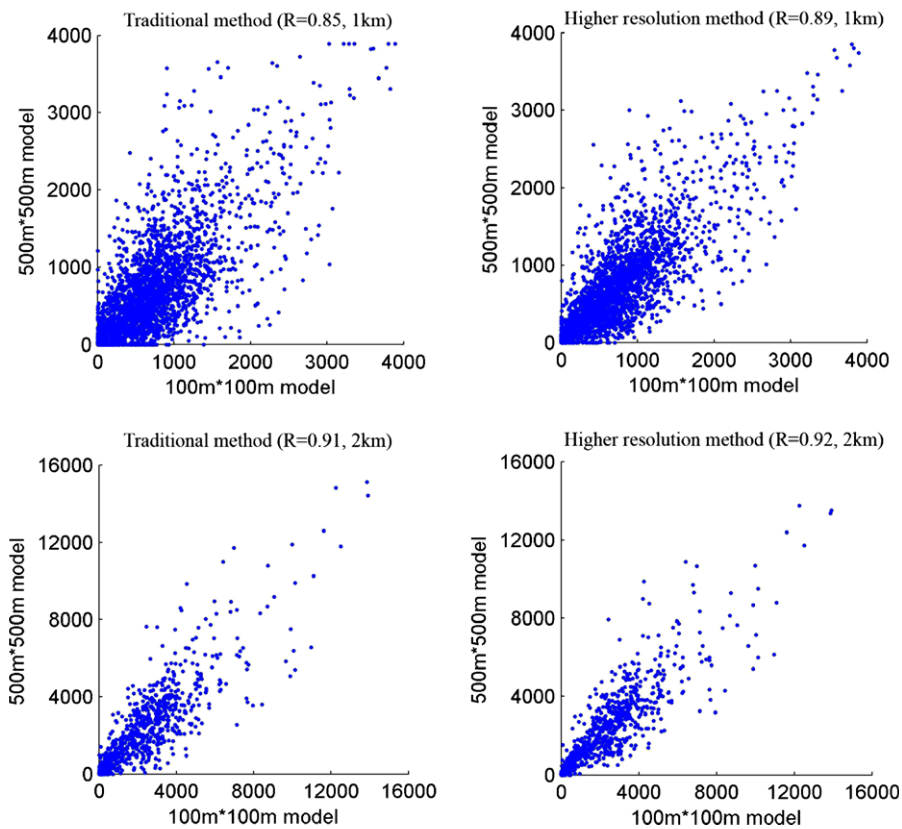

Figure 8 Comparison of evaporation rates ($m^3\,d^{-1}$ per cell) using the linear segment evaporation function on the basis of 1×1 km and 2×2 km cells. The evaporation rates on the *x*-axis are the sums of evaporation rates from the 100×100 m model for the corresponding 1×1 km and 2×2 km cells. The evaporation rates on the *y*-axis are the sum of evaporation rates from the 500×500 m model for the corresponding 1×1 km and 2×2 km cells (evaporation from the lake is not included).

modeling. The increase in correlation coefficient shows that already the expansion up to the second order correction yields substantial improvement compared to using the arithmetic mean of the elevations in the traditional method.

As we have seen in the comparison of evaporation with the linear segment evaporation function, the correlation is not very good on the basis of 500×500 m cells (the best being 0.81). It improves if we compare the evaporation rates on the basis of larger cells of 1×1 km and reaches 0.9 if we compare on the basis of 2×2 km cells. The exponential evaporation function leads to the same results (Fig. 10 and Table 3).

Conclusions and discussion

In this study, it is shown that the representation of the surface elevation in a groundwater model is important for the

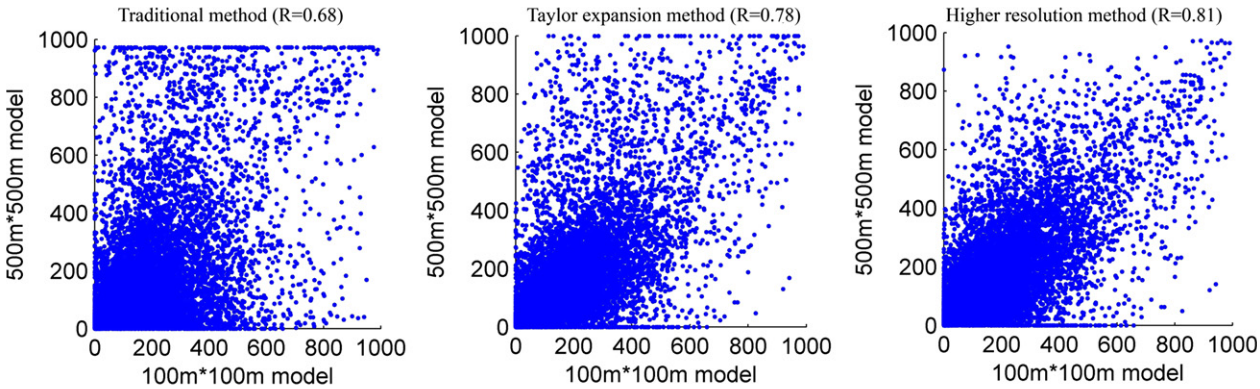

Figure 9 Comparison of evaporation rates (m^3 d^{-1} per cell) using the exponential evaporation function on basis of 500×500 m cells. The evaporation rates on the *x*-axis are the sum of evaporation results from the 100×100 m model for the corresponding cell in the 500×500 m model (evaporation from the lake is not included).

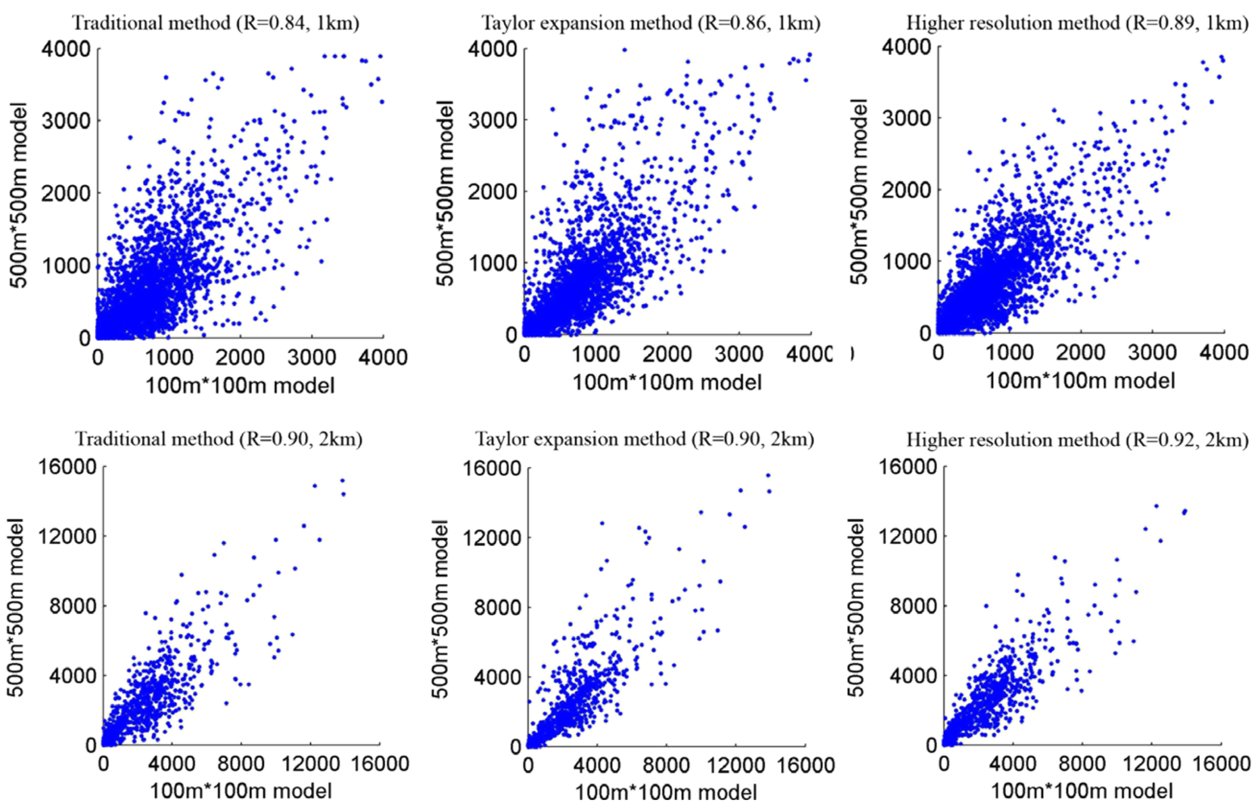

Figure 10 Comparison of evaporation rates (m^3 d^{-1} per cell) using the exponential evaporation function on the basis of 1×1 km and 2×2 km cells. The evaporation rates on the *x*-axis are the sum of evaporation rates from the 100×100 m model for the corresponding 1×1 km and 2×2 km cells. The evaporation rates on the *y*-axis are the sum of evaporation rates of the 500×500 m model for the corresponding 1×1 km and 2×2 km cells (evaporation from the lake is not included).

accuracy of spatial distribution of evaporation simulation. The evaporation is very sensitive to errors in the distance to groundwater caused either by inaccuracy of the surface elevation (after averaging) or of the computed heads. With this kind of error the individual cell values of evaporation rates in groundwater are very unreliable as is seen from the large scatter in the comparison of the assumed ''true'' evaporation rates from the 100×100 m model with the evaporation rates from the coarser 500×500 m model (see pictures on the left hand side of Figs. 7 and 9). While the point-wise comparison is unsatisfactory, the total evaporation rates in all cases are quite close (Tables 4 and 5). There are two important results of this study which show a way for improvement of evaporation calculation.

In any model, where the discretization is coarser than the resolution of the DEM available by an integer factor, the accuracy of evaporation simulation can be improved by taking the sub-cell elevation information into account instead of just specifying constant cell-wise elevation data for the corresponding model cell (the higher resolution

Table 4 Total evaporation rates using linear segment evaporation function (not including the evaporation of the lake)

	100 × 100 m model	500 × 500 m model	
		Traditional method	Higher resolution method
Total evaporation rates (10^6 m^3 d^{-1})	1.96	1.94	1.95

Table 5 Total evaporation rates using exponential evaporation function (not including the evaporation in the lake)

	100 × 100 m model	(500 × 500 m model)		
		Traditional method	Taylor expansion method	Higher resolution method
Total evaporation rates (10^6 m^3 d^{-1})	1.92	1.99	1.98	1.99

evaporation method in this study). This conclusion is true no matter which evaporation function is selected, the linear segment function or the exponential evaporation function.

The second way of improving the simulation is based on the observation that aggregation of evaporation rates over larger scales yields a smaller discrepancy between the ''true'' and the computed values. This means that errors cancel out when comparing on the basis of larger cells. Given the errors in depth to groundwater, the local evaporation result in a small cell has to be considered as a stochastic variable the aggregation of which in space leads to stable averages. In our example the aggregation over a 500 × 500 m cell is not yet sufficient to compare computed evaporation rates to ''measured'' ones. However, on the basis of 2 × 2 km cells the statistics of the sub-cell values are sufficient and a comparison appears feasible. It is crucial to represent the whole distribution of depths to groundwater in the cell used for comparison in order to remove bias. The experience from the field example used above can be generalized to all regions where the variation of the topographic elevation within a cell (or the error in topographic elevation) is on the same order as the extinction depth.

In this study, we only concentrate on evaporation simulation since it is a determining factor for the sustainable development in the research region. But the idea of taking sub-cell information into account can also be extended to other hydrological packages covering non-linear effects, e.g. recharge from rivers, etc.

Acknowledgments

We thank Christian Milzow at IfU, Richard B. Winston and George Z. Hornberger at USGS for generous help. We are also grateful for constructive comments by an anonymous reviewer and Wolfgang Schmid at Department of Hydrology & Water Resources, University of Arizona.

References

Alty, T., 1933. The maximum rate of evaporation of water. Philosophical Magazine 15 (96), 82–103.

American Society of Civil Engineers Task Committee on Hydrology Handbook, 1996. Hydrology Handbook. ASCE, New York, NY, 784pp.

Banta, E.R., 2000. MODFLOW-2000, the US Geological Survey modular ground-water model – documentation of packages for simulating evapotranspiration with a segmented function (ETS1) and drains with return flow (DRT1). US Geological Survey Open-File Report 00-466, 127p.

Barnes, C.J., Allison, G.B., 1988. Tracing of water-movement in the unsaturated zone using stable isotopes of hydrogen and oxygen. Journal of Hydrology 100 (1–3), 143–176.

Bauer, P., Held, R., Zimmermann, S., Linn, F., Kinzelbach, W., 2006. Coupled flow and salinity transport modeling in semi-arid environments: The Shashe River Valley, Botswana. Journal of Hydrology 316 (1–4), 163–183.

Brunner, P., 2005. Water and Salt Management in the Yanqi Basin, China, Ph.D. Dissertation. ETH Zurich No. 16210, ISBN: 3-906445-26-7. <http://e-collection.ethbib.ethz.ch/show?type=diss&nv=16210>.

Coudrain-Ribstein, A., Pratx, B., Talbi, A., Jusserand, C., 1998. Is the evaporation from phreatic aquifers in arid zones independent of the soil characteristics? Surface Geoscience 326, 159–165.

Craig, H., Gorden, L., 1965. Deuterium and oxygen-18 variations in the ocean and marine atmosphere. In: Tongiorgi, E. (Ed.), Stable Isotopes in Oceanographic Studies and Paleo-Temperatures, Pisa, pp. 9–130.

Gardner, W.R., 1958. Some steady state solutions of the unsaturated moisture flow equation with application to evaporation from a water table. Soil Science 85, 4.

Harbaugh, A.W., Banta, E.R., Hill, M.C., McDonald, M.G., 2000. MODFLOW-2000, the US Geological Survey modular ground-water model – user guide to modularization concepts and the ground-water flow process. US Geological Survey Open-File Report 00-92, 121p.

Hellweger, F., Maidment, D., 1997. AGREE – DEM Surface Reconditioning System.

Maddock III, T., Baird, K.J., 2003. A riparian evapotranspiration package for MODFLOW-96 and MODFLOW-2000. HWR No.02-03. Department of Hydrology and Water Resources, University of Arizona Research Laboratory for Riparian Studies, University of Arizona.

McDonald, M.G., Harbaugh, A.W., 1988. A modular three-dimensional finite difference ground-water flow model. US Geological Survey TWI 6-A1, 1988.

McDonald, M.G., Harbaugh, A.W., 1996. Programmer's documentation for MODFLOW-96, an update to the US Geological Survey modular finite-difference ground-water flow model. US Geological Survey Open-File Report 96-486.

Merritt, M.L., Konikow, L.F., 2000. Documentation of a computer program to simulate lake–aquifer interaction using the MODFLOW ground-water flow model and the MOC3D solute-transport model. US Geological Survey Water-Resources Investigations Report 00-4167, 146p.

Owens, J.S., 1934. Measuring rate of evaporation. Nature 134, 330.

Philip, J.R., 1957. Evaporation and moisture and heat fields in the soil. Journal of Meteorology 14, 354–366.

Rabus, B., Eineder, M., Roth, A., Bamler, R., 2003. The shuttle radar topography mission – a new class of digital elevation models acquired by spaceborne radar. Photogrammetric and Remote Sensing 57, 241–262.

Ripple, C.D., Rubin, J., van Hylkama, T.E.A., 1972. Estimating steady-state evaporation rates from bare soils under conditions of high water table. US Geological Survey Water Supp. Paper 2019-A.

Schmid, W., Hanson, R.T., Maddock III, T., Leake, S.A., 2006. User's guide for the farm process (FMP1) for the US Geological Survey's modular three-dimensional finite-difference ground-water flow model, MODFLOW-2000. US Geological Survey, Techniques and Methods Report 6-A17, 127p.

Wang, Z., 1990. Principles of Photogrammetry. Press of Wuhan Technical University of Surveying and Mapping, Beijing, China.

Zebker, H.A., Goldstein, R.M., 1986. Topographic mapping from interferometric synthetic aperture radar observations. Journal of Geophysical Research – Solid Earth and Planets. 91 (B5), 4993–4999.

Zimmermann, U., Ehhalt, D., Munnich, KO., 1967. Soil water movement and evapotranspiration: changes in the isotope composition of water. Isotopes in Hydrology, Vienna, 567–584.